

Interfacial structural characteristics and grain-size limits in nanocrystalline materials crystallized from amorphous solids

K. Lu

National Laboratory for RSA and International Center for Materials Physics, Institute of Metal Research, Academia Sinica, Shenyang 110015, People's Republic of China

(Received 25 July 1994)

The solid-state phase transformation from an amorphous solid into a nanocrystalline (NC) phase is studied from a thermodynamic point of view. The thermodynamic quantities of the interfaces (including the excess volume, excess energy, enthalpy, entropy, and the Gibbs free energy), which constitute a significant component in the NC materials, were calculated based on a quasiharmonic Debye approximation. By means of thermodynamic equilibrium conditions and quantitative calculations, we found that the structural characteristics of the interfaces are closely correlated with the grain-size limits crystallized from the amorphous phase. With a decrease in grain size, the excess volume as well as the excess energy of the interfaces formed during the crystallization will be reduced or, in other words, with the NC samples crystallized from the amorphous solids, a smaller grain size might be always associated with interfaces containing a smaller excess volume. This conclusion is in good agreement with experimental data of various systems for elements and alloys.

I. INTRODUCTION

Nanocrystalline (NC) materials are structurally characterized by ultrafine grains and a large volume fraction of interfaces, which enable many properties of the NC samples to be fundamentally different from and frequently superior to those of the conventional polycrystals.^{1,2} Therefore, this new class of materials has drawn increasing attention in recent years.

Up to now, several synthesis methods for the NC materials have been developed following the classical method of the *in situ* consolidation of ultrafine metal particles,^{1,2} for example, the ball-milling method,³ the electrodepositing method,⁴ the complete crystallization method from the amorphous solids,⁵ and so on. Among these synthesis routes, the complete crystallization method possesses some unique advantages:

(i) This method is very simple and convenient to control in preparation procedures. Conventional annealing can realize the nanocrystallization in most alloy and element systems providing they can be formed into amorphous states, and can produce a large quantity of the NC samples. Also, various grain sizes may be easily obtained in the NC specimens by modifying the heat treatment conditions.⁵

(ii) The complete crystallization method is an efficient way to produce porosity-free NC samples.⁶ Since no artificial consolidation process is involved and the nm crystallites and their boundaries are formed *via* solid-state phase transformation, the NC sample is dense and clean in the internal interfaces.

(iii) The nanocrystallization itself provides a unique opportunity to study the interface formation process from the amorphous state. The nanocrystallization kinetics and thermodynamics of the amorphous solids are strongly affected by the presence of plenty of interfaces in the crystallization products.^{7,8} Consequently, it is possible to

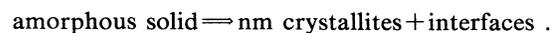
reveal some fundamental features of the interfaces in the NC materials from the transformation kinetic and thermodynamic signals.⁹

Because of these features, the complete crystallization method has been intensively investigated in the past few years. It has been successfully applied in various systems of both alloys and elements.^{5,10-20}

In this work, a thermodynamic analysis of the nanocrystallization process is performed in order to survey the influencing factors dominating the formation of nanometer-sized crystallites. By means of the thermodynamic equilibrium conditions and the quantitative calculations, we concluded that the structural characteristics of the interfaces are closely related to the grain-size limits. In the following sections, theoretical calculations and the correlation with the experimental results will be presented.

II. THERMODYNAMIC CONSIDERATIONS

The NC material consists of two structural components of (i) the nanometer-sized crystallites and (ii) grain boundaries or interfaces between the crystallites.¹ The volume fraction of the interfacial component will be much enhanced when the grain size is reduced to the nanometer scale. Then, the transformation from the amorphous phase into nanocrystalline phases may be considered as a "decomposition" of the amorphous phase into the nm crystallites and the interfaces, supposing the interface is regarded as a separated "phase" in the NC sample, i.e.,



The Gibbs free-energy change for the overall transformation may be expressed as follows if the interaction effect between the interfaces and the nm crystallites is negligible:

$$\Delta G(T) = (1 - x_i)\Delta G_f^c(T) + x_i\Delta G_f^i(T) - \Delta G_f^a(T), \quad (1)$$

where x_i is the atomic fraction of the interfaces in the NC sample, ΔG_f is the formation Gibbs free energy for different phases, and the superscript a =amorphous, c =nm crystallite, and i =interfaces. According to the thermodynamic equilibrium condition for a phase transformation, we may get a maximum value of the interfacial fraction when $\Delta G(T)=0$,

$$x_i^{\max}(T) = \frac{\Delta G_f^a(T) - \Delta G_f^c(T)}{\Delta G_f^i(T) - \Delta G_f^c(T)}. \quad (2)$$

The atomic fraction of the interface is inversely proportional to the average grain size (d), or $x_i \approx \alpha/d$ (where α is a constant relative to the thickness of the interface). Assuming the thickness of the interface is independent of the grain size, then the corresponding *minimum* grain size (d^*) is

$$d^*(T) = \frac{\alpha[\Delta G_f^i(T) - \Delta G_f^c(T)]}{\Delta G_f^a(T) - \Delta G_f^c(T)}. \quad (3)$$

According to the structure of crystallization products, three different cases may exist:

(I) Pure element nm crystallites. The simplest case is the transformation from an element amorphous phase (a - A) to an element nanocrystalline phase (NC- A). Taking approximately the element nm crystalline state as the thermodynamic standard state and $\Delta G_f^c=0$, we get

$$d^*(T) = \frac{\alpha\Delta G_f^i(T)}{\Delta G_f^a(T)}. \quad (3a)$$

(II) Single phase nm crystallites. When the crystalline products are of one crystalline phase, say, a compound of A_xB , there is

$$d^*(T) = \frac{\alpha[\Delta G_f^i(T) - \Delta G_f^{A_xB}(T)]}{\Delta G_f^a(T) - \Delta G_f^{A_xB}(T)}, \quad (3b)$$

where $\Delta G_f^{A_xB}$ is the formation Gibbs free energy for the nm-sized compound.

(III) Two or more nm-sized crystalline phases. The most common case in the crystallization of amorphous alloys is that the crystallization products contain two or more crystalline phases. Then,

$$d^*(T) = \frac{\alpha \left[\Delta G_f^i(T) - \sum_j x_j \Delta G_f^{c_j}(T) \right]}{\Delta G_f^a(T) - \sum_j x_j \Delta G_f^{c_j}(T)}, \quad (3c)$$

where $\Delta G_f^{c_j}$ is the formation Gibbs free energy for the j th nm-sized crystalline phase, and x_j is the molar fraction of the j th phase.

It can be seen from the above analysis that the grain-size limit is strongly dependent upon the Gibbs free energies of the three different states: the amorphous, the interfaces in the NC sample, and the crystalline phases(s). For simplicity in calculation, one might suppose the thermodynamic properties of the nm crystallites are approxi-

mately equal to those of the corresponding perfect crystals which are available from the classical thermodynamics theory, although some recent studies indicated that the microstructure of the nm crystallites is more or less different from that of the perfect crystal lattice.²¹⁻²³ Assuming $\Delta G_f^i(T) = \Delta G_f^c(T) - \Delta G_f^a(T)$, and $\Delta G^a(T) = \Delta G_f^a(T) - \Delta G_f^c(T)$, we simplified Eq. (3) to

$$d^* = \alpha \cdot \frac{\Delta G_f^i}{\Delta G^a}. \quad (4)$$

Evidently, ΔG_f^i and ΔG^a are the excess Gibbs free energies for the interface and the amorphous phases, respectively, related to the corresponding crystalline phase(s). In the following section, we demonstrate the determination of the excess Gibbs free energies for the amorphous phase and the interfaces.

III. CALCULATION AND RESULTS

A. Excess Gibbs free energy of the amorphous solid: ΔG^a

The thermodynamic properties of the amorphous solid can be approximated by those of a supercooled liquid state for $T \leq T_m$ (T_m is the melting temperature). Based on the classical thermodynamic theory, the excess enthalpy (ΔH^a), the excess entropy (ΔS^a), and the excess Gibbs free energy (ΔG^a) for the amorphous phase relative to the crystalline state are given as

$$\Delta H^a(T) = \Delta H_m - \int_T^{T_m} [C_p^a(T) - C_p^c(T)] dT, \quad (5)$$

$$\Delta S^a(T) = \Delta S_m - \int_T^{T_m} [C_p^a(T) - C_p^c(T)] d \ln T, \quad (6)$$

and

$$\Delta G^a(T) = \Delta H^a(T) - T\Delta S^a(T), \quad (7)$$

where ΔH_m =the melting enthalpy, ΔS_m =the melting entropy, $\Delta S_m = \Delta H_m/T_m$, and C_p^a and C_p^c are specific-heat capacities for the amorphous and the crystalline phases, respectively.

Different approximation models for $\Delta C_p(T) = C_p^a(T) - C_p^c(T)$ are well known. The first and the simplest approximation proposed by Turnbull²⁴ is $\Delta C_p = 0$. In this case, ΔG^a will be linearly (with a slope of $-\Delta S_m$) decreasing with an increase of temperature and $\Delta G^a = 0$ at $T = T_m$, as shown in Fig. 1.

Other ΔC_p approximations make the $\Delta G^a \sim T$ plot deviate from the straight line with $\Delta C_p = 0$. Jones and Chadwick²⁵ proposed $\Delta C_p(T) = \Delta C_p(T_m) = \Delta C_p^m$; Thompson and Spaepen²⁶ recommend $\Delta C_p(T) = \Delta H_m/T_m$, and Battezzati and Garrone²⁷ suggest $\Delta C_p(T) = 0.8\Delta H_m/T_m$. Dubey and Ramachandrarao²⁸ developed the following expression based on the hole theory of liquids:

$$\Delta C_p(T) = \Delta C_p^m \left[\frac{2T^3 + 3T^2\Delta T - \Delta T^3}{2T^3} \right] \quad (8)$$

with $\Delta T = T_m - T$. By using these approximations of $\Delta C_p(T)$, we calculated ΔG^a for a pure Ni, as shown in

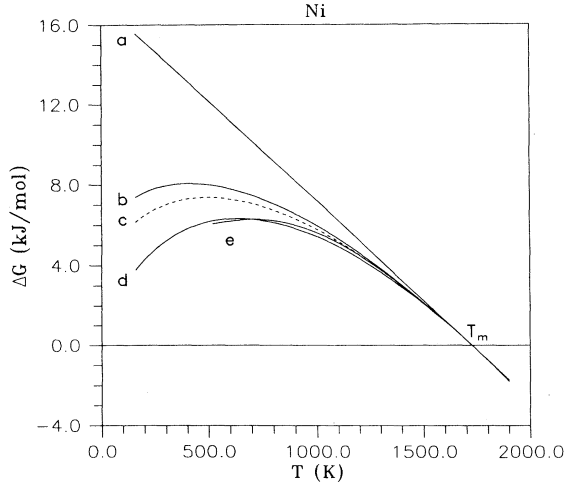


FIG. 1. Temperature dependences of the excess Gibbs free energy for the amorphous solid Ni calculated by using different ΔC_p models. (a) Turnbull's model (Ref. 24), (b) Jones and Chadwick's model (Ref. 25), (c) Battezzati and Garrone's model (Ref. 27), (d) Thompson and Spaepen's model (Ref. 26), (e) Dubey and Ramachandrarao's model (Ref. 28).

Fig. 1. It is clear that the later four models lead to the common feature that the $\Delta G^a \sim T$ lines are below the straight line with $\Delta C_p = 0$. The difference among them increases at lower temperature. However, the results from the four models (b, c, d, and e in Fig. 1) for $T \geq 0.5T_m$ are close, indicating that the difference among these ΔC_p models at that time is small.

B. Excess Gibbs free energy of the interface in the NC sample: ΔG^i

Determination of the excess Gibbs free energy of the interfaces in NC materials seems to be difficult as the thermodynamic properties for the interfaces are scarcely reported. The only thermodynamic property of the interfaces, which is available experimentally, is the interfacial energy. To obtain the thermodynamic parameters of the interfaces, therefore, we have to take a theoretical approach.

Theoretical calculations and simulations²⁹ indicated that the excess volume of a grain boundary, if compared to a single crystal, is found to be the most significant parameter to describe the grain-boundary energy, $\Delta V = V|V_0 - 1$ (where V and V_0 are the specific volumes for the boundary and the perfect crystal, respectively). In a grain boundary the number of nearest neighbors is reduced. A reduction of the number of nearest neighbors results in a decreased density of the system. Taking the density as the main feature of the grain boundary which is approximated by a perfect crystal lattice having an enhanced nearest-neighbor separation compared to the equilibrium atomic coordinations, we can calculate the thermodynamic properties of the grain boundary by estimating the properties of the corresponding dilated crystal. The calculation of the dilated crystal is carried out for a simple central force model in the quasiharmonic

Debye approximation.³⁰ It has been demonstrated by Wagner³¹ that some thermal properties of the NC metals (the specific-heat capacity and the thermal-expansion coefficient) approximated by using this model are in good agreement with experimental data.

According to the thermodynamic theory, the enthalpy change during a volume expansion from V_0 to V , corresponding to a negative hydrostatic pressure change from $P_0 = 0$ to P , is given as

$$\Delta H(T, V) = \Delta E(V) + \Delta[P(T, V) \cdot V], \quad (9)$$

where ΔE is the excess potential energy, $\Delta E(V) = E(V) - E(V_0)$. The potential energy is closely related to the nearest-neighbor distance, i.e., to the specific volume of the system, which can be expressed as

$$E = \frac{N}{2} \sum_{i \pm j} \varphi(|r_i - r_j|), \quad (10)$$

where $|r_i - r_j|$ is the distance between atom i and j . Taking the potential function as the Morse function,³⁰ we have

$$\varphi(r) = D[e^{-2b(r-a)} - 2e^{-b(r-a)}], \quad (11)$$

in which r is the nearest-neighbor distance, D , a , and b are the potential constants, which can be determined by means of the energy of sublimation and the coefficient of linear thermal expansion. Regarding only the nearest-neighbor interaction, Eq. (10) becomes

$$E = 6N\varphi(r). \quad (12)$$

The volume dependent hydrostatic pressure is $P(V) = -(\partial F / \partial V)_T$, where F is the Helmholtz free energy that is a function of temperature and volume. According to the quasiharmonic Debye approximation model, the Helmholtz free energy may be expressed as³⁰

$$F(T, V) = E + 3Nk_B T \ln(1 - e^{-\Theta/T}) - Nk_B T D(\Theta/T), \quad (13)$$

where N is the number of atoms, k_B is Boltzmann's constant, Θ is the Debye temperature which is a function of the volume, and

$$D(\Theta/T) = 3(T/\Theta)^3 \int_0^{\Theta/T} \frac{x^3}{e^x - 1} dx \quad (14)$$

is the Debye function.

As the pressure is given by $P = -(\partial F / \partial V)_T$, Eq. (13) leads to the equation of state:

$$P(T, V) = -\frac{\partial E / \partial r}{3cr^2} + \frac{3\gamma Nk_B T}{V} D(\Theta/T), \quad (15)$$

in which $V = cr^3$, c is a constant, for an fcc metal, $c = 1/\sqrt{2}$. γ is the Grüneisen parameter, which is a function of volume and related to the vibrational frequencies (ω) of phonons in metals as

$$\gamma = -(\partial \ln \omega / \partial \ln V)|_T. \quad (16)$$

In this simple model, the Debye temperature and the

Güneisen parameter only depend on the volume and are expressed as³²

$$\Theta(r) = \left[\frac{\varphi''(r)}{\varphi''(a)} \right]^{1/2} \Theta_0, \quad (17)$$

$$\gamma(r) = - \left[\frac{r}{6} \right] \left[\frac{\varphi''(r)}{\varphi''(r)} \right],$$

in which $\varphi''(r) = \partial^2 \varphi / \partial r^2$, $\varphi'''(r) = \partial^3 \varphi / \partial r^3$, Θ_0 is the Debye temperature for $r = a$, and $V = V_0 = ca^3$. As the Gibbs free energy (G) is related to the Helmholtz free energy (F) by $G = F + PV$, then

$$\Delta G(T, V) = \Delta F(T, V) + \Delta [P(T, V) \cdot V] \quad (18)$$

is the Gibbs free-energy change after the volume expansion, which might be thought of as the excess Gibbs free energy of the interfaces with an excess volume of ΔV .

For numerical calculation, a pure nickel system was chosen as an example. The potential constants are calculated to fit the energy of sublimation and the coefficient of linear thermal expansion: $D = 11.8 \times 10^{-20}$ J, $a = 2.5 \times 10^{-10}$ m, and $b = 1.35 \times 10^{-10}$ m⁻¹. The equilibrium Debye temperature of Ni is $\Theta_0 = 450$ K. Detailed calculation and analysis of the thermodynamic properties of the interfaces in pure Ni will be published elsewhere.³³

Figure 2 shows calculated results from the equation of state [Eq. (15)] for the interfaces in a pure Ni system. With an increase of the excess volume of the interface, the negative pressure increases before a critical value of the excess volume ΔV_c is reached when $P(V)$ has its negative maximum value corresponding to the bulk modulus of zero. Further expansion of the volume beyond ΔV_c would result in a negative bulk modulus thus violating the Gibbs stability criteria.³⁴ At the critical excess volume ΔV_c , the interface becomes mechanically unstable which is prevented by the formation of cracks during fur-

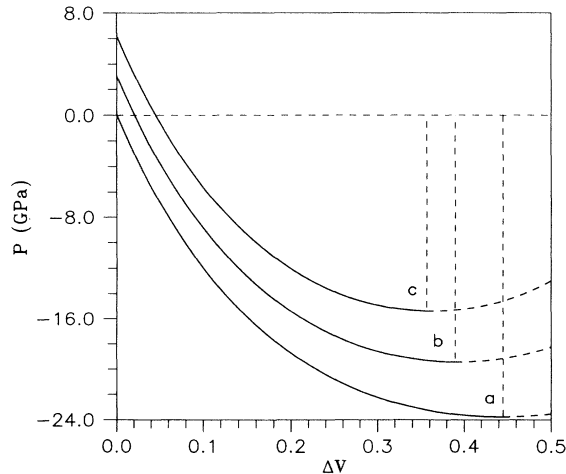


FIG. 2. Calculated results of dependences of the pressure on the excess volume of the interfaces in Ni at three parameters: (a) 300 K, (b) 800 K, and (c) 1300 K.

ther expansion. The value of ΔV_c is dependent on temperature, and the value of ΔV_c is larger at lower temperature, as can be seen in Fig. 2.

Figure 3(a) and 3(b) are calculation results of the excess energy (ΔE), excess enthalpy (ΔH), and the excess Gibbs free energy (ΔG), as functions of the excess volume at different temperatures. It is clear these three thermodynamic parameters increase monotonously with the expansion of the interface volume beyond the critical excess volume. The calculated dependence of ΔE on the excess volume in Ni, as presented in Fig. 3(a), is in a good agreement with the experimental observations in the Ni-P NC samples, with which we found the interfacial excess energy increases almost linearly with an increment of the excess volume of the Ni/Ni₃P interfaces.⁹ For the temperature dependent parameters, ΔH and ΔG , as shown in Fig. 3, the values increase steadily with increasing ΔV , whereas no stabilization effect (as described by Fecht³⁵ based on a model of the universal equation of state) is ob-

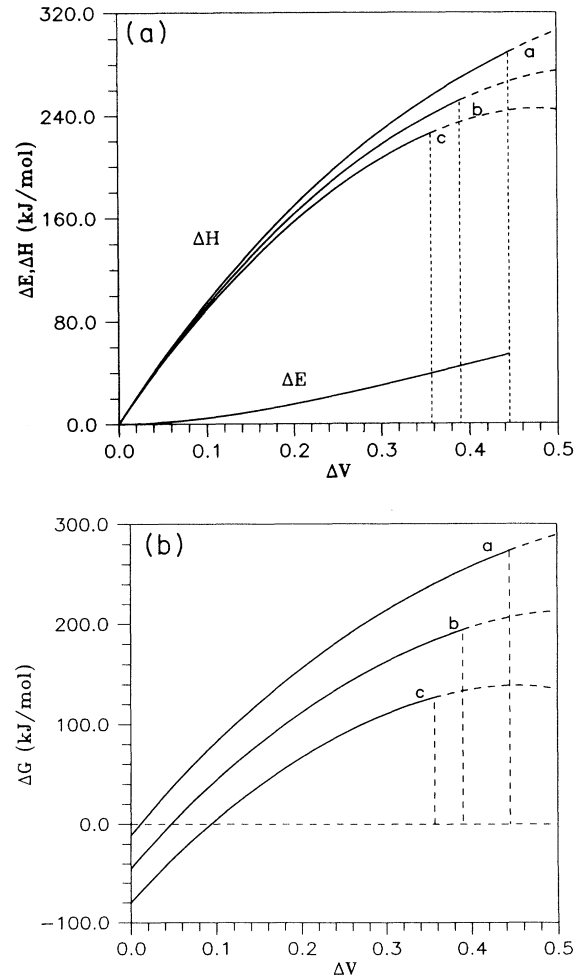


FIG. 3. Calculated results of the variations of the excess enthalpy (ΔH) and the excess energy (ΔE) (a), and of the excess Gibbs free energy (ΔG) (b), with the excess volume of the interfaces in Ni at three parameters: (a) 300 K, (b) 800 K, and (c) 1300 K.

served at any temperature. With a given excess volume, values of ΔH and ΔG are larger at higher temperatures.

The temperature dependences of the excess Gibbs free energy of the interface with different excess volumes are plotted in Fig. 4. It can be found that ΔG decreases in an approximate linear relation with increasing temperature for a given excess volume. With these results, it is possible to derive other thermodynamic properties of the interfaces.

C. Numerical calculations

Taking pure nickel as an example for the numerical calculations, we may use the results of ΔG for both the amorphous and the interfaces presented above to illustrate the grain-size limit crystallized from an amorphous solid. According to Eq. (4), the minimum grain size formed during crystallization of the amorphous phase is proportional to the ratio of $\Delta G^i/\Delta G^a$. Figure 5 shows the calculation results of $\Delta G^i/\Delta G^a$ versus temperature (T/T_m) with the interfaces containing different excess volumes of 10–30%. For the amorphous state, ΔG^a was calculated by means of the Battazatti's model of ΔC_p .²⁷ It can be seen from the calculations that with different excess volumes, the ratio of $\Delta G^i/\Delta G^a$ exhibits a slight variation with temperature in the range of 0.3–0.7 T_m . Or in other words, for an interface containing a certain excess volume, the ratio of $\Delta G^i/\Delta G^a$ is almost independent of temperature. As crystallization of amorphous alloys always occurs at temperatures around 0.5 T_m , it can be concluded that the grain-size limit d^* might not be a function of temperature providing the interfacial excess volume keeps constant.

Any change in the interfacial excess volume in the crystallization products would result in a significant variation in the grain-size limit. With an increase of the excess volume of the interfaces, ΔG^i will increase and ultimately lead to an increment of the grain size. Assuming the crystallizations take place at a temperature of 0.5 T_m ,

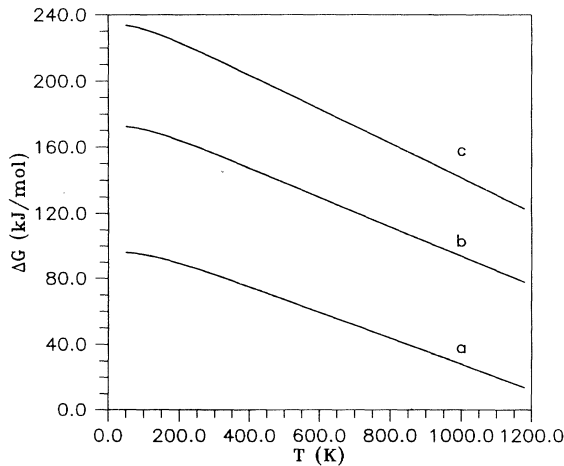


FIG. 4. Calculated results of the temperature dependence of the excess Gibbs free energy of the interfaces in Ni with different given excess volume: (a) 10%, (b) 20%, and (c) 30%.

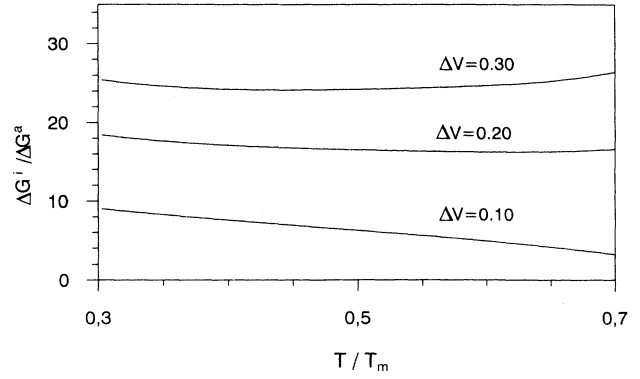


FIG. 5. Variation of the ratio $\Delta G^i/\Delta G^a$ with temperature with the interfacial excess volume of 10, 20, and 30%, respectively.

and the parameter α taken as 2.5, we may get a variation relationship between the excess volume of the interfaces and the grain-size limits during crystallization of an amorphous Ni, as shown in Fig. 6. Evidently, the calculated result indicates that an increase in the excess volume of the interfaces would result in an increase of the grain-size limit. Or reversely, when the grain size in the crystallization products is increased, the interface formed must contain larger excess volumes.

It should be mentioned that the above calculations should be valid for other systems of elements and alloys containing a single phase in the crystallization products. In the case of alloys in which the crystallization products consist of two or more phases, the same results might be obtained if the excess Gibbs free energy of the interface can be approximated by

$$\Delta G^i(T) = \left[\Delta G_f^c(T) - \sum_j x_j \cdot \Delta G_f^{c_j}(T) \right].$$

Consequently, an universal conclusion may be derived from the thermodynamic considerations that a smaller grain size in the crystallization products of amorphous solids is always associated with a denser internal interface formed during the transformation.

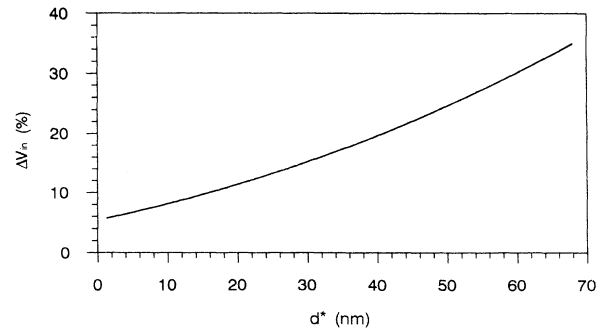


FIG. 6. The calculated result of the relationship between the interfacial excess volume and the grain size limit for the NC materials crystallized from the amorphous states.

IV. EXPERIMENTAL EVIDENCE

A complete crystallization from the amorphous solid into nanocrystalline phases has been realized in many systems, ranging from elements to various Ni-, Fe-, and Co-based alloys. Although detailed investigations on the interfacial structures in the NC samples synthesized *via* a complete crystallization are still in progress, there is some solid experimental evidence which may support the conclusion drawn from the thermodynamic analyses.

A. Quantitative results of the interfacial excess volume and interfacial excess energy in the Ni-P alloy nanophases with different mean grain sizes

The crystallization of an amorphous Ni₈₀P₂₀ (at. %) alloy is a typical eutectic crystallization process, resulting in formation of two crystalline phases of a Ni(P) solid solution and a Ni₃P compound. An increase in the annealing temperature leads to an enlargement of the average grain size from a few to more than 100 nm.⁹ Density measurements and the positron annihilation spectroscopy studies revealed that the density of the interfaces formed in the NC Ni-P samples increases with the decreased grain size. Namely, the excess volume of the interfaces is decreased with a reducing grain size.³⁶ As plotted in Fig. 7, the measurement results show that the excess volume of the interfaces decreases from about 28% (when $d = 68$ nm) to only 8% (when $d = 7.5$ nm).

By means of a microcalorimetric measurement of the amorphous-to-NC transformation, the interfacial excess energy was derived in the NC Ni-P samples with different grain sizes. It was found that with a reduction of grain size, the interfacial excess energy decreases linearly, which correlates well with the decreasing tendency of the interfacial excess volume, and hence reconfirms the $\Delta V \sim d$ variation tendency. This feature of decreasing interfacial excess energy with a reduction of grain size has been successfully used in explanation of the abnormal Hall-Petch relationship in the NC materials.³⁷

With the thermodynamic analysis presented in the Sec.

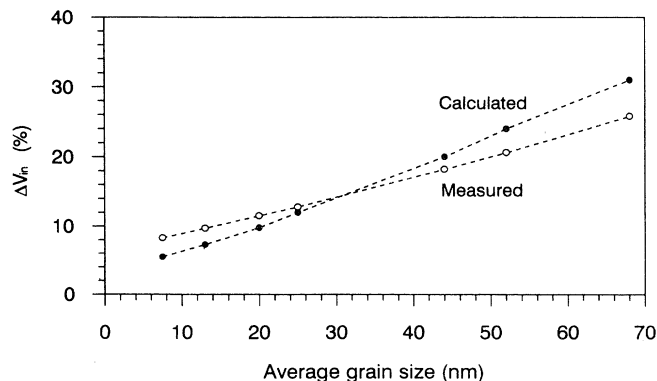


FIG. 7. Measured and calculated results of the relationship between the interfacial excess volume and the average grain size in the Ni-P NC materials crystallized from the amorphous alloy.

III C, one may also calculate the interfacial excess volume in the NC samples by using the measured data of the average grain size and annealing temperature in the Ni-P system. Supposing the structure of the interfaces in the NC Ni-P samples, most of which are the Ni Ni₃P interphase boundaries, is approximately identical to that in the pure Ni case, we get a variation relation of $\Delta V \sim d$ according to Eq. (4), as plotted in Fig. 7. It can be seen the calculated results are in a satisfactory agreement with the experimentally measured ones.

B. Positron annihilation spectroscopy results in the Ni-P and Fe-Si-B nanophase samples

Positron annihilation lifetime spectroscopy has been used in investigations on the variation of the interfacial defects with grain size in the Ni-P and Fe-Si-B nanophase samples crystallized from the amorphous states, respectively.^{6,38} In both cases it was found there are only two lifetime components, a short lifetime component τ_1 and an intermediate τ_2 , corresponding to two kinds of interfacial defects, respectively: type-I of free volumes of which the size is smaller than a monovacancy, and type-II of microvoids, of which the type-I is in the overwhelming majority. With a decrease in the mean grain size, there are more type-I defects and less type-II in a unit area of the interfaces, exhibiting a significant increment in the intensity ratio of the two components (I_1/I_2), as shown in Fig. 8. That is to say, the density of the interfaces increases with a reduction of the grain size in the nanophase samples, which agrees well with the quantitative results of the variational relationship of the interfacial excess volume and excess energy with the mean grain size in the Ni-P samples.

C. Effect of the structure of the original amorphous state on the grain-size limit

From the thermodynamic analyses one may imagine that the original structure of the amorphous phase would affect the resultant crystallization products. From Eq. (4), it is clear that an increase in the excess Gibbs free energy for the amorphous phase may reduce the grain-size limit in the crystallization products. Tong *et al.*³⁹ have examined the effect of the amorphous structure on the grain size in the Fe-B-Si alloy. In their work, four different amorphous samples were prepared by using the single-roller spinning technique, where different quenching rates were obtained by changing the rotating speed of the wheel. It was found with a decrease of the line speed of the rotating wheel (i.e., a decrease of the quenching rate) from 41.5 to 17.0 m/s, the minimum grain size in the crystallization products increases from about 25 to about 70 nm, as shown in Fig. 9, while the crystallization products contain the same structure of a Fe(Si) solid solution and a Fe₃B compound. An increase in the quenching rate would enhance the degree of amorphism, and consequently raise the excess Gibbs free energy for the amorphous state. Therefore, this result provides direct support to the theoretical analysis that the grain-size limit is closely related to the state of the amorphism providing the interfacial structure remains unchangeable.

D. Minimum grain sizes in the three types of crystallization processes

Usually, crystallization of amorphous solids may be classified into three types according to the transformation mechanism: polymorphous, eutectic, and primary crystallization.⁴⁰ During nanocrystallizations, these three types of mechanisms have also been detected in different alloy systems, respectively. Analyzing experimental results on the complete crystallization into NC materials, we may find the interesting phenomenon that the minimum grain sizes are always small (a few nm) for the polymorphous and the eutectic crystallizations, while for the primary

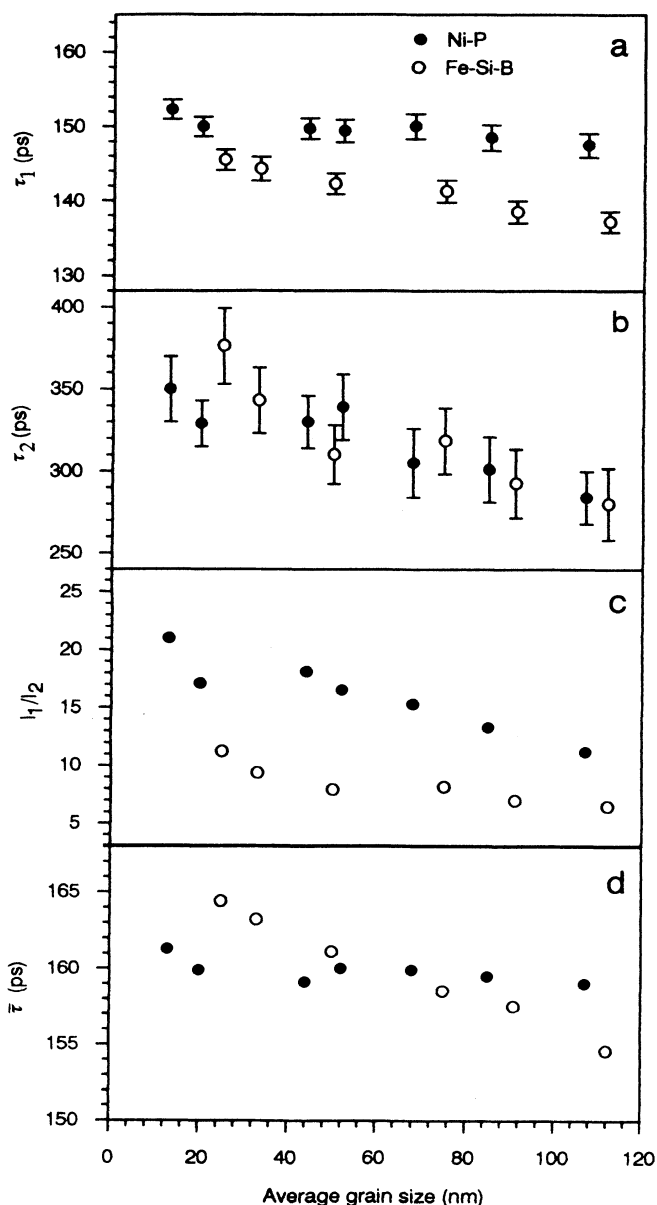


FIG. 8. Plots of the position lifetime results of NC Ni-P (Ref. 6) and Fe-Si-B alloys (Ref. 38) versus the average grain size. The intensity ratio (I_1/I_2) reflects the interfacial excess volume.

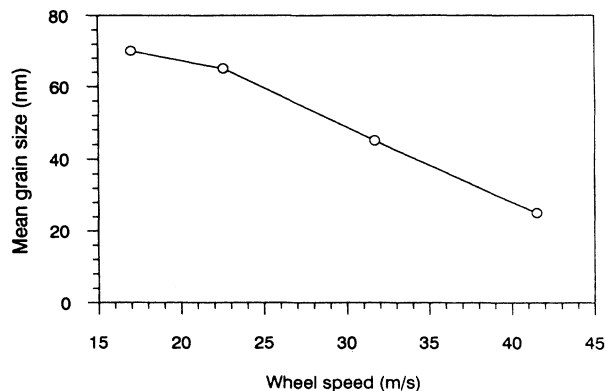


FIG. 9. Measurement results of the mean grain sizes in the crystallization products from the amorphous Fe-Si-B alloys quenched with different wheel speeds (i.e., different quenching rates) (Ref. 39).

crystallization products the minimum grain sizes are large (15–30 nm). Tables I–III compile the experimental results of the minimum grain sizes in several systems published in the literature for the polymorphous, eutectic, and primary crystallizations. It should be noted that some data in these tables, such as in the Fe-B⁴¹ and Fe-Ni-P-B alloys,⁴² are taken from early work dealing with the interphase spacings in the crystallization products, which are actually a measure of the average grain size. From these results we may see the minimum grain size is almost independent of the number of alloy elements. Such a difference in the minimum grain sizes due to different crystallization mechanisms may provide us some hints for the structural characteristics of the interfaces formed during nanocrystallization processes.

Different crystallization mechanism may produce interfaces with different microstructures. For the polymorphous and the eutectic nanocrystallizations, as the overall composition of the crystallization products keeps the same as that of the matrix amorphous phase, these two kinds of transformation processes are controlled by the interface movement, and no composition pileup could be built in front of the growing crystals. The polymorphous crystallization produces a single phase, where fine microdomains or microtwinned textures are frequently formed,⁴³ which is referred as to the nanocrystalline grains. For example, in the NiZr₂ glass, the crystallization product is highly twinned. The NC grains are characterized by the following orientation relation:

TABLE I. Experimental data of the minimum grain sizes (d^*) and the annealing temperature (T_a) in the polymorphous nanocrystallization.

System	Crystalline phase(s)	d^* (nm)	T_a/T_m	Ref.
Si	α -Si	7.0–8.0	0.50	48
Se	γ -Se	6.7–7.8	0.76	19
Co ₃₃ Zr ₆₇	CoZr ₂	8.0	0.50	10
Ni ₃₄ Zr ₆₆	NiZr ₂	8.0–10.0	0.49	20
(Fe,Co) ₃₃ Zr ₆₇	(Fe,Co)Zr ₂	4.0–5.0	(773 K)	11

TABLE II. Experimental data of the minimum grain sizes (d^*) and the annealing temperature (T_a) in the eutectic nanocrystallization.

System	Crystalline phase(s)	d^* (nm)	T_a/T_m	Ref.
Ni ₈₀ P ₂₀	Ni ₃ P + Ni(P)	6.0–7.0	0.50	5
Fe ₈₀ B ₂₀	Fe ₃ B + Fe(B)	8.0	0.46	41
Fe ₄₀ Ni ₄₀ P ₁₄ B ₆	(FeNi) ₃ (PB) + FeNi(PB)	9.0	0.55	42

$[001]_1 || [111]_2$ and $[110]_1 || [110]_2$.⁴⁴ The grain boundaries between the nanometer-sized grains are always in low energetic configurations, exhibiting either twin boundary or small-angle coherent boundary, and therefore containing very small excess volume.

For the eutectic crystallization, two crystalline phases crystallize simultaneously, between them there is always a defined orientational relationship. For example, in the crystallization products of the Ni-P system, the orientation relationship between Ni phase and Ni₃P compound is $\langle 001 \rangle_{\text{bct}} || \langle 110 \rangle_{\text{fcc}}$ and $\langle 110 \rangle_{\text{bct}} || \langle 111 \rangle_{\text{fcc}}$.⁴⁵ This orientation relationship indicates the interfaces of Ni/Ni₃P may be coherent or semicoherent, of which the excess energy would be small, as confirmed by the calorimetric measurements of the interfacial energies in the NC Ni-P samples.⁴⁶

Comparatively, the primary crystallization creates a different interface structure. During a primary crystallization, a primary phase may be formed with random orientations and distributed randomly inside the amorphous matrix. Because the crystallization of a primary phase is controlled by diffusion process, there is a compositional pileup in front of the growing crystals. In the second stage of crystallization, the residual amorphous phase crystallizes into two or more phases in the form of heterogeneous nucleation and growth process. The interfaces formed in such a primary crystallization might be in a higher energetic state relative to those formed in the other crystallization mechanism. According to the theoretical analysis presented in Sec. III C, the higher energetic state of interfaces, and hence containing larger excess volumes, might be the intrinsic reason for the larger grain-size limits in the primary nanocrystallization than those in the polymorphous and the eutectic ones.

From the literature data of positron annihilation lifetime spectroscopy measurements in various kinds of

nanophase alloys, which underwent different crystallization processes, one may also find some differences in the interfacial defects. A comparison of the measurement results for three kinds of nanocrystallization products was listed in Table IV. For the eutectic system, say, the Ni₈₀P₂₀ nanophase sample, the ratio of I_1/I_2 which represents the relative amount of the type-I defects in the interfaces is about 21.0, and the mean lifetime $\bar{\tau} = (\tau_1 \cdot I_1 + \tau_2 \cdot I_2) / (I_1 + I_2)$ is about 160.0 ps, which is only about 8 ps higher than the lifetime component for the amorphous Ni-P sample (151.9 ps). But for the primary nanocrystallization products, such as in the Fe-Si-B (Ref. 38) and the Fe-Mo-Si-B (Ref. 47) nanophase samples, the ratio of I_1/I_2 is around 11.0 and the mean lifetimes are about 14 ps larger than that of the amorphous state. These results indicate that for the eutectic crystallization products, there are more type-I defects and less type-II in the interfaces, i.e., the interfaces are relatively denser compared with those in the primary crystallization products.

V. DISCUSSION AND CONCLUSIONS

The above analyses and discussions are concentrated on the thermodynamic aspects. Concerning the crystallization kinetics of amorphous solids, one may also find a significant effect of the interfacial structure on the kinetic process, and consequently, on the crystallization products. In most cases, a crystallization of an amorphous phase is considered as a combination process of nucleation and growth of crystalline phases. In principle, formation of ultrafine grains during a crystallization is favored with a high nucleation rate and a low growth rate, and/or with a small critical nucleus size during the transformation. In classical nucleation theory the steady-state homogeneous nucleation rate I_{st} is given by

$$I_{\text{st}} = I_0 \exp \left[\frac{-Q}{RT} \right] \exp \left[\frac{-L \Delta G_c}{RT} \right], \quad (19)$$

where I_0 is a pre-exponential factor, L is the Loschmidt number, Q is the activation energy for the transfer of atoms across the surface of the nucleus which is approximately equal to the diffusion activation energy, and ΔG_c is the free energy required to form a nucleus of the critical size, which can be written as

TABLE III. Experimental data of the minimum grain sizes (d^*) and the annealing temperature (T_a) in the primary nanocrystallization.

System	Crystalline phase(s)	d^* (nm)	T_a/T_m	Ref.
Fe ₇₈ B ₁₃ Si ₉	Fe(Si) + Fe ₃ B	21–25	0.51	12
Fe ₆₀ Co ₃₀ Zr ₁₀	Fe(Co) + (FeCo) ₂ Zr	15	0.51	13
(Fe ₉₉ Mo ₁) ₇₈ B ₁₃ Si ₉	Fe(Si,Mo) + (FeMo) ₃ Si + Fe ₂ B	17–20	0.52	14
(Fe ₉₉ Cu ₁) ₇₈ B ₁₃ Si ₉	Fe(Si) + Fe ₂ B	27	0.50	15
Pd _{78.1} Cu _{5.5} Si _{16.4}	Pd(Si) + (PdCu) ₃ Si	19	0.62	49
Fe _{74.5} Nb ₃ B ₉ Si _{17.5}	Fe(Si) + Fe ₂₃ B ₆	18	0.53	16
Fe _{73.5} Cu ₁ Ta ₃ B ₉ Si _{13.5}	Fe(Si) + Fe ₃ B	70	(790 K)	17
Fe ₈₆ Cu ₁ B ₆ Zr ₇	Fe(Si) + Fe ₂ B	16	(793 K)	18

TABLE IV. Literature data of the positron annihilation spectroscopy results for different nanophase alloys which underwent three different crystallizations.

Crystallization	Sample	d^* (nm)	τ_1 (ps)	τ_2 (ps)	I_1/I_2	$\bar{\tau}$ (ps)	τ_a (ps)
Eutectic	Ni ₈₀ P ₂₀ (Ref. 6)	7.0	152.3±1.3	350±20	21.0	160.0	151.9
Primary	Fe ₇₈ Si ₉ B ₁₃ (Ref. 38)	25	145.5±1.4	376±23	11.3	164.2	150.8
	(Fe ₉₉ Mo ₁) ₇₈ Si ₉ B ₁₃ (Ref. 47)	20	139.4±1.5	240±12	10.7	165.8	151.2

$$\Delta G_c = \frac{16\pi\gamma^3}{3\Delta G_v^2}, \quad (20)$$

where ΔG_c is the Gibbs free-energy difference between the crystal and the matrix amorphous phase, and γ is the interfacial energy of the crystal/glass interfaces. The critical nucleus size r_c is

$$r_c = \frac{2\gamma T_m}{\Delta H_v \Delta T}, \quad (21)$$

in which ΔH_v is the enthalpy change for the transformation, $\Delta T = T_m - T$ is the undercooling. From these equations, it is known that at a given temperature high nucleation rates can be only achieved if the nucleation barrier ΔG_c is small, i.e., if the driving force for the crystallization ΔG_v is large and/or the interfacial energy γ is small. And the critical nucleus size will be also decreased if the interfacial energy becomes smaller. The grain boundary in the crystallization products, to some extent, could represent the structure characteristics of the crystal/glass interfaces during the crystallization, which is actually a precursor of the grain boundaries in the products.

While for the growth rate of a crystalline nucleus, according to the crystal-growth theory, the driving force for grain growth is proportional to the interfacial energy. Therefore, the growth rate of crystalline nucleus will be dramatically reduced if the interfacial energy is lowered. The grain size in a crystallization is proportional to the square root of a ratio, $(u/I_{st})^{0.5}$. It is clear that a decrease in the interfacial energy (i.e., a decrease in the excess volume of the crystal/glass interfaces) will result in a

significant refinement of the grain size. This agrees with the thermodynamic analyses.

From the experimental results of the polymorphous and the eutectic nanocrystallization products, one may find that the minimum grain sizes obtained in these alloy systems are always small (less than 10 nm). According to the theoretical calculations (as to Fig. 6), it is reasonable to believe that the interfacial excess volume in the as-crystallized NC samples should be very small (less than 10%). Hence, an important implication might result from the comparison between the experimental and the theoretical results, that both the eutectic and the polymorphous crystallization can lead to NC materials containing densified interfaces with a very low excess energy.

Finally, it can be concluded that the structural characteristics of the interfaces are closely correlated with the grain-size limits during the nanocrystallization from the amorphous solids. With a decreased grain size, the excess volume and the excess energy for the interfaces in the crystallization products will be reduced. Or in other words, for the NC materials crystallized from an amorphous solid, smaller grain size may be obtained when the interfacial excess volume is smaller and/or the degree of amorphism of the original amorphous state is higher.

ACKNOWLEDGMENTS

The financial support from the Chinese Academy of Sciences and the National Science Foundation of China is acknowledged. The author thanks Dr. X. D. Liu and Mr. J. Xu for their helpful suggestions and discussions.

¹H. Gleiter, *Prog. Mater. Sci.* **33**, 223 (1989); R. Birringer, U. Herr, and H. Gleiter, *Trans. Jpn. Inst. Met. Suppl.* **27**, 43 (1986).
²R. W. Siegel, in *Physics of New Materials*, edited by F. E. Fujita, Springer Series in Materials Sciences, Vol. 27 (Springer-Verlag, Berlin, 1994), p. 65.
³C. C. Koch, *Nanostruct. Mater.* **2**, 109 (1993).
⁴U. Erb, A. M. El-Sherik, G. Palumbo, and K. T. Aust, *Nanostruct. Mater.* **2**, 383 (1993).
⁵K. Lu, J. T. Wang, and W. D. Wei, *J. Appl. Phys.* **69**, 522 (1991); *Scr. Metall. Mater.* **24**, 2319 (1990).
⁶M. L. Sui, K. Lu, W. Deng, L. Y. Xiong, S. Patu, and Y. Z. He, *Phys. Rev. B* **44**, 6466 (1991); *J. Appl. Phys.* **69**, 4451 (1991).
⁷R. Lück, K. Lu, and W. Frantz, *Scr. Metall. Mater.* **28**, 1071 (1993); K. Lu, R. Lück, and B. Predel, *J. Alloys Compounds* **201**, 229 (1993).

⁸K. Lu, R. Lück, and B. Predel, *Acta Metall. Mater.* **42**, 2303 (1994).
⁹K. Lu, R. Lück, and B. Predel, *Scr. Metall. Mater.* **28**, 1387 (1993).
¹⁰M. M. Nicolaus, H.-R. Sinning, and F. Haessner, *Mater. Sci. Eng. A* **150**, 101 (1992).
¹¹T. Spassov and U. Köster, *J. Mater. Sci.* **28**, 2789 (1993).
¹²H. Y. Tong, J. T. Wang, B. Z. Ding, H. G. Jiang, and K. Lu, *J. Non-Cryst. Solids* **150**, 444 (1992).
¹³H. Q. Guo, T. Reininger, H. Kronmüller, M. Rapp, and V. Kh. Skumrev, *Phys. Status Solidi A* **127**, 519 (1991).
¹⁴X. D. Liu, J. T. Wang, and X. D. Liu, *Scr. Metall. Mater.* **28**, 59 (1993).
¹⁵X. D. Liu, K. Lu, B. Z. Ding, and Z. Q. Hu, *Chinese Sci. Bull.* **39**, 27 (1994).
¹⁶F. Zhou, K. Y. He, *et al.* (unpublished).

- ¹⁷T. Kulik, T. Horubala, and H. Matyja, *Mater. Sci. Eng. A* **157**, 107 (1992).
- ¹⁸P. Gorria, I. Orue, F. Plazaola, and J. M. Barandiaran, *J. Appl. Phys.* **73**, 6600 (1993).
- ¹⁹H. Y. Zhang, K. Lu, and Z. Q. Hu, *Acta Phys. Sinica* (to be published).
- ²⁰K. Lu, X. D. Liu, F. H. Yan, and W. D. Wei (unpublished).
- ²¹K. Lu and M. L. Sui, *J. Mater. Sci. Tech.* **9**, 419 (1993).
- ²²M. L. Sui and K. Lu, *Mater. Sci. Eng. A* **179/180**, 541 (1994).
- ²³X. D. Liu, K. Lu, Z. Q. Hu, and B. Z. Ding, *Nanostruct. Mater.* **2**, 581 (1993).
- ²⁴D. Turnbull, *J. Appl. Phys.* **21**, 1022 (1950).
- ²⁵D. R. H. Jones and G. A. Chadwick, *Philos. Mag.* **24**, 995 (1971).
- ²⁶C. V. Thompson and F. Spaepen, *Acta Metall.* **27**, 1855 (1979).
- ²⁷L. Battezzati and E. Garrone, *Z. Metallkd.* **75**, 305 (1984).
- ²⁸K. S. Dubey and P. Ramachandrarao, *Acta Metall.* **32**, 91 (1984).
- ²⁹D. Wolf, *Philos. Mag. B* **59**, 667 (1989).
- ³⁰L. A. Gerifalco and V. G. Weizer, *Phys. Rev.* **114**, 687 (1959).
- ³¹M. Wagner, *Phys. Rev. B* **45**, 635 (1992).
- ³²P. Brüesch, *Phonons: Theory and Experiments I*, Solid-State Sciences, Vol. 34 (Springer-Verlag, Berlin, 1982).
- ³³K. Lu, *Acta Phys. Sinica* (to be published).
- ³⁴H. J. Rose, J. R. Smith, F. Guinea, and J. Feerante, *Phys. Rev. B* **29**, 2963 (1988).
- ³⁵H. J. Fecht, *Acta Metall. Mater.* **38**, 1927 (1990).
- ³⁶M. L. Sui and K. Lu, *Acta Metall. Sinica* **30**, B121 (1994).
- ³⁷K. Lu and M. L. Sui, *Scr. Metall. Mater.* **28**, 1387 (1993).
- ³⁸H. Y. Tong, B. Z. Ding, J. T. Wang, K. Lu, J. Jiang, and J. Zhu, *J. Appl. Phys.* **72**, 5124 (1992).
- ³⁹H. Y. Tong, B. Z. Ding, *et al.* (unpublished).
- ⁴⁰U. Herold and U. Köster, in *Glassy Metals I*, edited by H. J. Guntherodt and H. Beck, (Springer-Verlag, New York, 1981), p. 225.
- ⁴¹A. L. Greer, *Acta Metall.* **30**, 171 (1982).
- ⁴²D. G. Morris, *Acta Metall.* **29**, 1213 (1981).
- ⁴³M. G. Scott, in *Amorphous Metallic Alloys*, edited by F. E. Luborsky (Butterworth, London, 1983), p. 144.
- ⁴⁴C. Beeli, H.-U. Nissen, Q. Jiang, and R. Lück, *Mater. Sci. Eng. A* **133**, 346 (1991).
- ⁴⁵M. L. Sui, K. Lu, and Y. Z. He, *Philos. Mag. B* **63**, 933 (1991).
- ⁴⁶K. Lu, W. D. Wei, and J. T. Wang, *J. Appl. Phys.* **69**, 7345 (1991).
- ⁴⁷X. D. Liu, B. Z. Ding, and J. T. Wang, *J. Mater. Sci. Lett.* **12**, 1826 (1993).
- ⁴⁸Y. L. He and X. N. Liu, *Acta Electron. Sinica* **4**, 70 (1982).
- ⁴⁹P. G. Boswell and G. A. Chadwick, *Scr. Metall.* **70**, 509 (1976).